Behavioral/Cognitive

Spatiotemporal Dynamics of Successive Activations across the Human Brain during Simple Arithmetic Processing

Pedro Pinheiro-Chagas,[1,2] Clara Sava-Segal,[1]* Serdar Akkol,[1]* Amy Daitch,[1] and Josef Parvizi[1]

[1]Stanford Human Intracranial Cognitive Electrophysiology Program, Department of Neurology and Neurological Science, Stanford University, Stanford, California 94305 and [2]UCSF Memory and Aging Center, Department of Neurology, Weill Institute for Neurosciences, University of California, San Francisco, California

Previous neuroimaging studies have offered unique insights about the spatial organization of activations and deactivations across the brain; however, these were not powered to explore the exact timing of events at the subsecond scale combined with a precise anatomical source of information at the level of individual brains. As a result, we know little about the order of engagement across different brain regions during a given cognitive task. Using experimental arithmetic tasks as a prototype for human-unique symbolic processing, we recorded directly across 10,076 brain sites in 85 human subjects (52% female) using the intracranial electroencephalography. Our data revealed a remarkably distributed change of activity in almost half of the sampled sites. In each activated brain region, we found juxtaposed neuronal populations preferentially responsive to either the target or control conditions, arranged in an anatomically orderly manner. Notably, an orderly successive activation of a set of brain regions—anatomically consistent across subjects—was observed in individual brains. The temporal order of activations across these sites was replicable across subjects and trials. Moreover, the degree of functional connectivity between the sites decreased as a function of temporal distance between regions, suggesting that the information is partially leaked or transformed along the processing chain. Our study complements prior imaging studies by providing hitherto unknown information about the timing of events in the brain during arithmetic processing. Such findings can be a basis for developing mechanistic computational models of human-specific cognitive symbolic systems.

Key words: brain dynamics; dyscalculia; electrocorticography; intracranial EEG; mathematical cognition; symbolic systems

Significance Statement

Our study elucidates the spatiotemporal dynamics and anatomical specificity of brain activations across >10,000 sites during arithmetic tasks, as captured by intracranial EEG. We discovered an orderly, successive activation of the brain regions, consistent across individuals, and a decrease in functional connectivity as a function of temporal distance between regions. Our findings provide unprecedented insights into the sequence of cognitive processing and regional interactions, offering a novel perspective for enhancing computational models of cognitive symbolic systems.

Introduction

Past studies in humans and nonhuman primates have provided an important information about regional activations during arithmetic processing (Brannon, 2006; Ansari, 2008; Cantlon et al., 2009; Butterworth and Walsh, 2011; Dehaene, 2011; Cohen Kadosh and Dowker, 2015; Nieder, 2019; Knops, 2020). More specifically, neuropsychological and neuroimaging studies

have uncovered a static and coarse functional map of activations in the brain, which in the context of arithmetic processing, includes a network of regions within the posterior parietal cortex (PPC), presumably engaged in numerosity representation and manipulation (Dehaene et al., 1999; Piazza et al., 2007; Knops et al., 2009; Holloway and Ansari, 2010; Harvey et al., 2013; Kanjlia et al., 2016), and the ventral temporal cortex (VTC), presumably involved in the recognition of numerical symbols (Shum et al., 2013; Grotheer et al., 2016a,b; Amalric and Dehaene, 2017; Grotheer et al., 2018). The engaged PPC sites are further grouped into at least three functionally diverse subregions (Dehaene et al., 2003): the horizontal portion of the intraparietal sulcus (IPS), which is strongly engaged during number comparison (Piazza et al., 2007) and calculation (De Smedt et al., 2011); the superior parietal lobe (SPL), which hosts a topographical representation of quantities (Harvey et al., 2017) and is involved in visuospatial processing and orienting of attention during calculation

(Knops et al., 2009; Mathieu et al., 2017; Liu et al., 2021); and the left angular gyrus, which is suggested to be involved in verbal number processing such as multiplication fact retrieval (Delazer et al., 2003; Grabner et al., 2009; see also Grabner et al., 2013; Pinheiro-Chagas et al., 2022). Performing a simple arithmetic calculation would therefore depend on an interplay between different subregions of the PPC, between PPC and VTC, and between these regions and other auxiliary brain regions that are required for performing executive functions and working memory (e.g., dorsolateral prefrontal cortex), declarative and semantic memory formation (e.g., medial temporal lobe), and the allocation of attentional resources for goal-directed problem-solving (e.g., various prefrontal cortical regions).

While we have learned a great deal of information from the extant evidence, our knowledge has been primarily based on the group-averaged correlational data that could not simultaneously resolve the spatial and temporal dynamics of the activity at the individual brain level. As a result, the precise anatomical location, temporal dynamics of activity, and how these regions collaboratively work together to perform calculations are still poorly understood. This is partially due to the low temporal resolution and low signal-to-noise ratio of signals obtained with noninvasive neuroimaging methods. While the lower temporal resolution of fMRI precludes assessments of fast spatiotemporal dynamics across these sites, the lower signal-to-noise ratio of M/EEG often requires a group-based analysis that blurs the anatomical precision of the data at the single-subject level.

In the past few years, studies using intracranial electroencephalography (iEEG) have provided several novel findings that are advancing our understanding of the spatiotemporal dynamics of processing in the human brain. While the iEEG method is not suited for fine-grained studies of neuronal activity at the local level, it is a remarkable tool for the simultaneous recording of averaged neuronal population activities across remote regions of the brain (Parvizi and Kastner, 2018). Using this method, our group has confirmed the existence of a specialized area in the posterior inferior temporal gyrus (pITG) in the human VTC that selectively responds to numerals as compared with other morphometrically and semantically similar symbols (Shum et al., 2013). Subsequent studies have shown that the pITG sites are functionally connected with neuronal populations around the IPS, found to be associated with magnitude representation and manipulation (Daitch et al., 2016; Pinheiro-Chagas et al., 2018), and modulated by arithmetic problem size (Kanjlia et al., 2016; Pinheiro-Chagas et al., 2018). A further study demonstrated that responses in the pITG during calculation are format independent (i.e., equal responses for numerals and number words; Baek et al., 2018). These results have suggested that the pITG may be involved in functions beyond digit recognition. Although our recent iEEG studies provided precise information about the anatomical location and temporal dynamics of activity between the VTC and IPS hubs of activity, they were only focused on a single pair of brain regions and relied on observations in a small number of subjects—due to the rarity of recordings in these areas of the brain.

In the current study, we leveraged the power of multisite iEEG recordings across a relatively large number of human subjects. Crucially, several of our subjects had simultaneous recordings across the key regions of the brain known to be involved during the mathematical processing. This allowed us to investigate the spatiotemporal dynamics of arithmetic processing at the single-subject level and with single-trial precision. We had several

predictions based on previous studies. Based on the neuropsychological data showing the heterogeneity of behavioral deficits following focal (Baldo and Dronkers, 2007) and network brain lesions (Gorno-Tempini et al., 2011), we hypothesized the existence of juxtaposed neuronal populations with preferential responses for math and non-math tasks. Extending our prior work to a larger number of regions (Daitch et al., 2016; Pinheiro-Chagas et al., 2018; Baek et al., 2018), we predicted that sites with a high degree of preferential response to math processing will show a particular signature of activity profile, which can be observed as a sharp increase in activation following the calculation stage of the task. Complementarily, we expected to observe an antagonistic pattern of deactivation across regions of the default mode network at a similar processing stage, which has never been demonstrated. Lastly, expanding our previous findings with just a few electrodes (Daitch et al., 2016), we predicted the existence of a canonical temporal order of activations along the math network, following regions in the ventral temporal, lateral parietal, and dorsolateral prefrontal cortices. In addition to these specific hypotheses, our study was poised to gain novel insights into the precise anatomical organization within individual brains, the temporal dynamics, and the functional connectivity during arithmetic calculations. Our findings have the potential to serve as a foundational platform for developing mechanistic computational models of human-unique cognitive abilities, thus greatly advancing our understanding of mathematical cognition.

Materials and Methods

Participants. We recorded intracranial electroencephalography (iEEG) data from 85 human subjects (52% females; Extended Data Fig. 1-1, Subject's demographics, basic neuropsychological information, and task completion) with medically refractory epilepsy who were implanted with intracranial electrodes as a part of their presurgical evaluation at Stanford University. Each subject provided an informed consent to participate in the study, which was approved by the Stanford Institutional Review Board. The subjects were monitored for ~6–10 d following surgery, during which they participated in our study. The electrode location and number were determined by the neurosurgeons for clinical needs. The data from 16 subjects of the present cohort was already published previously (Shum et al., 2013; Daitch et al., 2016; Hermes et al., 2017; Baek et al., 2018; Pinheiro-Chagas et al., 2018).

Electrophysiology recording. A total of 39 cases were implanted with subdural grids (ECoG), 45 with depth electrodes (stereoelectroencephalography, sEEG), and 3 with both sEEG and ECoG, whose locations were determined purely for clinical reasons. For depth electrodes (stereo-EEG), the diameter was 0.86 mm, the height was 2.29 mm, and the distance between the centers of two adjacent electrodes was 5 mm. For subdural grids and strips (ECoG) electrodes, the diameter was usually 2.3 mm with a center-to-center interelectrode spacing of 10 mm, 7 mm, or 5 mm for higher density arrays. All electrodes were from AdTech Medical Instruments.

Data acquisition and analysis. iEEG data were recorded using two multichannel recording system: Tucker David Technologies (bandpass filter of 0.5–300 Hz and sampling rate of 1,525.88 Hz or 3,051.76 Hz) or Nihon Kohden (sampling rate 1,000 Hz). After data collection, we implemented a preprocessing pipeline to minimize noise in the electrophysiological signals. Initially, signals above 1,000 Hz were downsampled to 1,000 Hz. We then applied notch filters at 60, 120, and 180 Hz to the downsampled signals to remove electrical line noise. Subsequently, we identified and excluded the noisy channels from further analyses. These were defined as channels with raw amplitude exceeding five times or falling below one-fifth of the median raw amplitude across all channels or those exhibiting more than three times the

median number of spikes across all channels (spikes were defined as jumps between consecutive data points >80 μV). We also excluded electrodes whose overall power was five or more standard deviations above or below the mean power across channels and those whose power spectrum deviated from the normal $1/f$ power spectrum, based on visual inspection. Electrodes marked by the clinical team as having an epileptiform activity were also excluded from subsequent analyses, along with the noisy electrodes. All nonexcluded channels were then notch filtered at 60 Hz and harmonics to remove the electric interference and then rereferenced to the mean of the filtered signals of the nonexcluded channels. The rereferenced signal at each electrode was then bandpass filtered between 70 and 180 Hz (high-frequency broadband, HFB) using sequential 10 Hz width bandpass windows (70–80 Hz, 80–90 Hz, etc.), using two-way, zero-lag, finite impulse response filters. The instantaneous amplitude of each band-limited signal was computed by taking the modulus of the Hilbert transform signal. The amplitude of each 10 Hz band signal was normalized by its own mean, and then these normalized amplitude time series were averaged together, yielding a single amplitude time course for the HFB band. The data were analyzed using the Matlab R2020_b with a custom-made pipeline: https://github.com/pinheirochagas/lbcn_preproc.

All analyses were conducted at the level of individual electrodes, and a subset [response onset latency (ROL), functional connectivity, and feature modulation] were done at the single-trial level. The group analyses were conducted at the second level, incorporating the information computed at the trial and electrode levels. This approach allowed us to maintain the high resolution of our data while also enabling us to draw broader conclusions across subjects and regions. Of note, while parametric tests are widely used in the analysis of electrophysiological data (Kiebel et al., 2005), we used nonparametric tests when we analyzed the data across electrodes in case the condition of independence across electrodes and ROIs could not be fully met.

Electrode localization. We used the iELVis toolbox in order to localize electrodes (Groppe et al., 2017). All subjects had preimplantation T1-weighted MRI and postimplantation CT scans following the electrode implantation. T1-weighted MRI scan was used to generate cortical surface and subcortical segmentation using recon-all command of the FreeSurfer v6.0.0 (Fischl et al., 1999). The postimplant CT scan was aligned to the preimplant MRI using the *flirt* from the Oxford Centre for Functional MRI of the Brain Software Library (Jenkinson and Smith, 2001; Jenkinson et al., 2002) or using *bbregister* from FreeSurfer (Greve and Fischl, 2009) to get the best results. We then manually labeled each electrode on the T1-registered CT image using the BioImage Suite (Papademetris et al., 2006). For subdural grid and strip electrodes (but not for depth electrodes), we used one of two brainshift correction methods in order to get the closest results to the intraoperative pictures (Dykstra et al., 2012; Yang et al., 2012). To combine data across subjects, electrodes were meticulously determined by a highly trained neuroanatomist, J.P., who considered the anatomical landmarks and morphology of individual brains. Importantly, the neuroanatomist was completely blind to the results.

Functional preferentiality. Our analyses were focused on task-induced changes in the HFB activity (70–180 Hz), due to its high correlation with local spiking activity and the fMRI BOLD signal (Logothetis et al., 2001; Ray and Maunsell, 2011). Additionally, the HFB signal is proven to have sufficient anatomical resolution to capture independent activity from each electrode, even when multiple electrodes are located within the same grid or brain region (Ray and Maunsell, 2011; Dubey and Ray, 2019). This is based on the understanding that the HFB signal reflects localized neural processes and can vary significantly across closely spaced electrodes. However, we acknowledge that this is a complex issue and that some degree of spatial autocorrelation may exist in the data due to shared inputs or local network effects (Parvizi and Kastner, 2018).

We classified all sites based on their relative responses during target (arithmetic) versus control (memory) trials. Math-involved sites were defined as those with a significantly different HFB activity during arithmetic trials compared with the prestimulus baseline period (see below). If the trial HFB activity was higher than baseline, we considered the site

math active, and if the trial HFB activity was lower than baseline, we considered the site math deactivated. Math preferential sites were defined as those that satisfied the three criteria: (1) significantly higher trial HFB compared with baseline; (2) significantly greater trial HFB activity during math compared with the non-math condition (autobiographical memory/language); and (3) no significant difference in trial HFB activity during the non-math condition as compared with baseline. Math and non-math active sites were defined as those with significantly higher trial HFB compared with baseline in both math and non-math conditions and with no significant difference in the trial HFB activity between math and non-math conditions. Non-math involved, non-math active, non-math deactivated, and non-math preferential were classified using equivalent criteria. The trial and baseline periods for the comparisons used in the simultaneous calculation task were 100–1,000 ms following the stimulus presentation and −200 to 0 ms before stimulus presentation, respectively. The trial window was selected not only because all necessary information for performing the calculation (in the math condition) or retrieving the memory (in the non-math condition) is presented simultaneously but also because this 1 s window is where the majority of the signal was concentrated. For the sequential calculation task, the trial and baseline periods were 2,100–4,300 ms following the first stimulus and −500 to 0 ms before the first stimulus, respectively.

On the other hand, the sequential calculation task has a different structure with the information presented in a staggered manner. Consequently, the trial window for this task is longer (2,200 ms) and begins 100 ms after the presentation of the third stimulus. This timing allows subjects to gather all the necessary information before starting the calculation or memory retrieval process. The varying baseline durations were chosen based on the intertrial interval, which was 200 ms for the simultaneous task and 500 ms for the sequential task. This procedure ensured that the baseline period did not overlap with any task stimuli.

Note that this is not circular to the response profile findings (Figs. 2. 3), since the analysis comparing the HFB within different stages of calculation was performed post hoc to the functional preferentiality analysis. Unpaired permutation tests were run to test for differences in HFB power between different task conditions, while paired permutation tests were run to test for a difference in HFB power between a task condition and baseline. All *p* values in all analyses were FDR corrected by the total number of sites within each subject, using the procedure introduced by Benjamini and Hochberg (1995).

ROL analysis. Based on our previously published methods (Schrouff et al., 2018), we implemented a method to estimate the onset of the task-induced trial-by-trial HFB response at each site. We first normalized the signal to the peak amplitude and applied a sliding window with 30 ms bins with 28 ms overlap. We then calculated the signal average and standard deviation in a baseline time window of [−200, 0] ms before onset across trials in each condition. We then identified 25 consecutive bins in which the average HFB power *z* score was one standard deviation above the baseline average. The earliest time point of the first bin in this sequence was marked as the onset for a specific trial. All analyses were done on a trial-by-trial basis. Sites in which the ROL could not be calculated for >50% of the trials were discarded from the analysis.

Cross-correlation. For each pair of electrodes, we ran a cross-correlation analysis (function xcorr in Matlab) with max lag of [−2, 2] s from the stimulus onset in the simultaneous calculation task. Next, we randomly shuffled the trial order and recalculated the cross-correlation. We repeated this process 2,000 times and subtracted the averaged permuted shuffled trial order from the averaged Pearson's *r* trace from the preserved trial order. If two regions are functionally connected, the difference between ordered minus shuffled trials (Δr_{peak}) should be high and positive. And if one region A is leading and another region B is lagging, the lag of the peak (Δr_{lag}) should be positive.

Simultaneous calculation task. The subjects were presented with visual stimuli that were either math statements (arithmetic calculations, i.e., "48 + 5 = 57") or non-math statements (autobiographical memory, i.e., "I ate fruit yesterday"). The subjects were instructed to make true/false

judgments about each statement or equation by pressing two keypad buttons. Each arithmetic statement (addition) was always composed of a two-digit operand (ranging from 10 to 87), a single-digit operand (ranging from 1 to 9), and a two-digit proposed result. In half of the trials, the proposed result was correct. The task was self-paced, but the subjects had maximum of 15 s to make these judgments. A 200 ms intertrial period separated the trials. The trials were interspersed with fixation periods (5 s), during which the subjects were simply asked to fixate at a cross-hair in the center of the screen. The subjects completed approximately two blocks. Each block had 80 trials (40 math and 40 non-math, randomly sampled from the stimuli list), which lasted ~15 min. Stimuli were not repeated across blocks. Within each block, math and non-math statements were presented in a randomized order (Extended Data Fig. 1-2, Stimuli list for the simultaneous calculation task for the full list of stimuli).

Sequential calculation task. The subjects were presented with a series of visual stimuli that were either math statements or non-math statements, like the ones presented in the simultaneous calculation task. The subjects were instructed to make true/false judgments about each statement or equation by pressing two keypad buttons. Each stimulus within a statement was presented one numeral/symbol/word at a time (i.e., "1" "+" "2" "=" "3"; "I" "ate" "fruit" "yesterday"). Half of the math trials were presented as math symbols ("1 + 2 = 3") and half using words ("one plus two equals three"). In half of the math trials, the proposed result was correct. Each stimulus was presented for 500 ms with a 500 ms interstimulus period. After the last stimulus was presented, the subjects had 5 s to respond. A 500 ms of intertrial period separated the trials. The subjects completed between two and four blocks. Each block consisted of 48 trials (24 math and 24 non-math, randomly sampled from the stimuli list), lasting ~10 min. Stimuli were not repeated across blocks. Within each block, math and non-math statements were presented in a randomized order. See Extended Data Figure 1-2, Stimuli list for the simultaneous calculation task for the full list of stimuli.

We chose the distinction math versus non-math, because for this paper we were not particularly focused on the precise cognitive functions underlying the non-math condition beyond their lack of involvement in math; a similar terminology has been adopted in our recent studies. The non-math statements essentially represent a reading task with autobiographical memory content (Amalric and Dehaene, 2016, 2017).

Results

Subjects and recording electrodes
We recruited 85 subjects with focal epilepsy implanted with intracranial electrodes as part of their presurgical evaluation. The electrodes were implanted in these subjects solely for clinical reasons, and the subjects were monitored in private hospital rooms for 1–2 weeks. Our research studies were performed while the subjects were comfortably resting in their hospital bed during their clinical monitoring. A total of 10,076 recording sites were included: 56% in the left hemisphere and 56% (ECoG) throughout the last 12 years. The subjects performed simple arithmetic sums presented in two different methods: in the first experiment, also referred to as Task 1 or "simultaneous calculation," the subjects judged the accuracy of full math statements (arithmetic equations, e.g., "16 + 8 = 22") or full non-math statements (autobiographical memory, e.g., "Today, I had a beer") that appeared in randomized order on a computer screen. In the second task, that is, Task 2, or "sequential calculation," the subjects viewed similar statements but with items presented serially or one at a time (e.g., "Today," "I" "had" "a beer" or "16", "+", "8", "=", "22"; Fig. 1a).

Behavioral performance
The subjects demonstrated high performance in the math and non-math conditions for both the simultaneous and sequential tasks. We classified trials as incorrect when subjects got the answer wrong or when they had extreme response times (RTs) (<200 ms or >10 s

for the simultaneous and >5 s for the sequential task math condition), since that suggested either a lack of attention or engagement. For the simultaneous math condition, the subjects accurately responded to 84.9% of the trials (SD, 13.11%), with a mean RT, 3,723 ms, and SD, 1,283 ms (RT calculated from onset of full statement). For the sequential math condition, the subjects accurately responded to 83.8% of the trials (SD, 8.4%), with a mean RT, 1,332 ms, and SD, 495 ms (RT calculated from the onset of the last item, i.e., "22" in "16 + 8 = 22"). In the sequential non-math condition, since these involved subjective questions, accuracy could not be assessed. However, the RT for the simultaneous non-math condition was mean, 2,635, and SD, 956, and for the sequential non-math condition, it was mean, 1,652, and SD, 471. A statistical analysis revealed significant RT differences between the math and non-math conditions across both tasks. In simultaneous tasks, responses were slower in math condition by 1,088 ms, $t_{(68)} = 5.65$, $p < 0.0001$. In contrast, the subjects were faster for the math condition in the sequential tasks by 320 ms, $t_{(53)} = 3.44$, $p < 0.001$. Incorrect trials were excluded from all further analyses.

To model RTs, we calculated stepwise regression models for each participant with several arithmetic features that are classically associated with problem difficulty as predictors. Take a proposed problem like "7 + 35 = 44": the min operand is the smallest operand ("7"); the max operand is the largest operand ("35"); the cross-decade is true, since the correct result "42" lies on the decade "40" that is different from the one of the max operand which is "30"; the magnitude order is either smaller operand + larger operand or larger operand + smaller operand (which was only possible to model in the simultaneous calculation task, because all stimuli of the sequential calculation task were larger operand + smaller operand); the format is a digit (in the sequential calculation task, it can also be number words, such as "seven plus thirty five equals forty four"); and the absolute deviant is the modulus of the difference between the correct ("42") and proposed ("44") results, which in this case is "2". In the simultaneous calculation task, results revealed that the cross-decade variable was overall the best predictor of RT (significant in 46 subjects, 70%), followed by min operand (significant in 36 subjects, 55%), absolute deviant (significant in 28 subjects, 42%), max operand (significant in 11 subjects, 17%), and magnitude order (significant in 9 subjects, 14%). In the sequential calculation task, we found that the best predictor of RT was the min operand (significant in 17 subjects, 65%), followed by format (significant in 15 subjects, 58%), absolute deviant (significant in 12 subjects, 46%), cross-decade (significant in five subjects, 19%), and max operand (significant in three subjects, 12%).

These behavioral results corroborate previous findings using a variety of paradigms, such as verification, production, and number to position, in which the min operand and cross-decade are consistently found to be good predictors of RT (Groen and Parkman, 1972; Barrouillet and Thevenot, 2013; Uittenhove et al., 2016; Pinheiro-Chagas et al., 2017), thus providing a convergent evidence that these arithmetic features are robust and reproducible indices of problem difficulty.

Functional anatomical organization
To investigate which sites were engaged during the math condition, we calculated the band-limited power of signals that recorded in the HFB (70–180 Hz, normalized to the prestimulus baseline) as a reliable measure of "regional engagement"—as reviewed previously (Parvizi and Kastner, 2018).

By comparing the HFB activity during the calculation stage against the prestimulus baseline period in all 10,076 recording
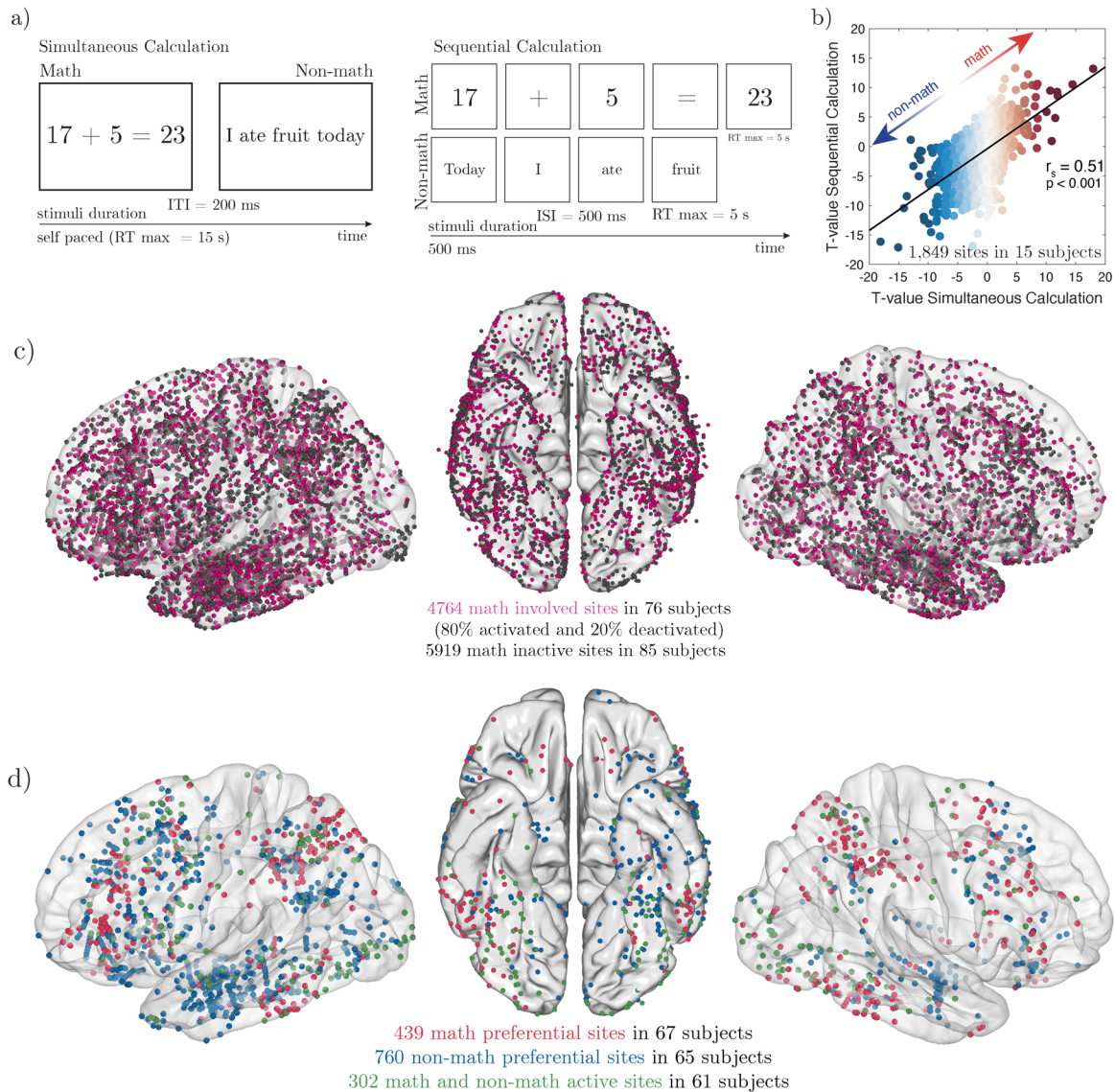
Figure 1. *a*, Design of the simultaneous and sequential calculation tasks. *b*, Correlation of the *T* value from the comparison between math and non-math averaged activity in each site from all the 15 subjects who completed both tasks. *c*, Electrode coverage combining all 10,076 recording sites across 85 subjects plotted on a common brain (fsaverage). Each black dot represents one electrode. Most electrodes (62%) were ECoG and located on the left hemisphere (59%). *d*, Selectivity map for math and non-math (autobiographical memory/language) across all electrodes during the simultaneous and sequential calculation tasks combined. Electrodes are colored by selectivity: math preferential in red, non-math preferential in blue, and sites equally activated for both math and non-math in green. See Extended Data Figures 1-1–1-8.

sites across 85 subjects, we identified that 4,764 sites (45%) were significantly involved during arithmetic calculations (Fig. 1*c*). These sites were distributed throughout the entire mantle of the cerebral cortex in both hemispheres. Out of these involved sites, 3,811 (80%) were significantly activated (i.e., poststimuli activity increased as compared with the baseline period; see Materials and Methods), and 953 (20%) were significantly deactivated (i.e., poststimuli activity decreased as compared with the baseline period; Fig. 4).

As noted, the main goal of the current study was to study the dynamics of engagement and interaction across neuronal populations located in different regions of the brain during arithmetic processing. To address this aim, we focused our analysis on a selected set of brain regions that displayed the highest degree of activations during the arithmetic trials. In line with neuroimaging studies, we identified the sites in each subject that exhibited significant activations (i.e., HFB responses) compared with baseline

and higher activations during the math condition compared with non-math condition. It is important to note that this does not imply that the selected sites were engaged strictly in arithmetic computation per se. Instead, this subtractive approach (activity during math compared with activity during non-math control condition) was used to make our analyses similar to the ones employed in the majority of neuroimaging studies and to identify brain regions where peaks of activations are found.

Across all subjects, we identified 439 sites (9.21%, in 67 subjects) with preferential activity during math as compared with the non-math condition (Fig. 1*d*). The *t* scores from the comparison of induced HFB power during math compared with those during non-math conditions were highly correlated when calculated from Task 1 and Task 2 (i.e., simultaneous vs sequential calculation; $r = 0.55$; $p < 0.001$; $df = 1,848$; $n = 15$ subjects; 1,849 recording sites; Fig. 1*b*). This clearly suggests that the preferential responses in these sites were driven by the task content (i.e.,

arithmetic calculation) rather than by the task structure or demand.

Math preferential sites could be dissociated from the set of anatomical regions with preferential responses during non-math ($N = 760$ in 65 subjects). The anatomical location of the sites with preferential activation during arithmetic processing was remarkably consistent across task formats (i.e., in both simultaneous and sequential tasks) and across individual brains. We selected nine regions of interest for a deeper analysis based on the following criteria: (1) regions that have been implicated in mathematical processing in previous fMRI and neuropsychological studies and (2) regions that contained a substantial number of electrodes (i.e., $n > 10$), prioritizing the simultaneous calculation task, given the significant coverage and emphasis on this task in our study. We acknowledge that this selection process may seem arbitrary, and we understand that despite the extensive nature of our database, it is not feasible to investigate all brain regions with the same level of precision. The selected ROIs were as follows: fusiform gyrus (FG); inferior temporal gyrus (ITG); IPS; SPL; supramarginal gyrus (SMG); inferior (IFG), middle (MFG), and superior frontal gyrus (SFG); and medial superior frontal gyrus (mSFG; Fig. 2). In each of these broad regions, we could find both math and non-math–preferential neuronal populations. However, consistent anatomical relationships could be observed between math and non-math activated sites. To confirm that, we conducted Spearman's rank correlation between the T value of the comparison between math and non-math and the electrode's coordinate in the native individual anatomical space, using the coordinate axis that best captured this relationship. We found

that functional preference was organized in these regions. In the FG, math-responsive sites were located primarily in the right hemisphere, while non-math–activated sites were located predominantly in the left hemisphere. Moreover, the math-activated sites were located more lateral to non-math sites in the ITG; more posterior to non-math sites in the SPL, SFG, and mSFG (although the correlation for mSFG did not survive the FDR correction for multiple comparisons); more anterior to non-math sites in the IPS, MFG, and IFG; and more dorsal to non-math sites in the SMG (Fig. 2).

Profile of activity across anatomical regions
By leveraging the temporal resolution and the high signal-to-noise ratio of the iEEG signal, we explored the pattern of electrophysiological changes within a given neuronal population from the time of stimulus onset to the time of subject's responses. During Task 1, when arithmetic equations were presented at once, sites with preferential responses during the arithmetic condition exhibited a similar profile of sustained responses. During Task 2, in which the arithmetic stimuli were presented sequentially, we discovered a stereotyped signature of activation across sites. Neuronal population responses in math-preferential sites were significantly higher after operand and response conditions (e.g., "2" and "3" and "5" in "2 + 3 = 5") as compared with arithmetic operation symbols (e.g., "+" and "=" in "2 + 3 = 5"). Interestingly, the activity induced by the second operand was also significantly higher than the activity induced by the first operand. This is noteworthy because after the first operand and first operation symbol (e.g., "2" and "+" = in the above example),
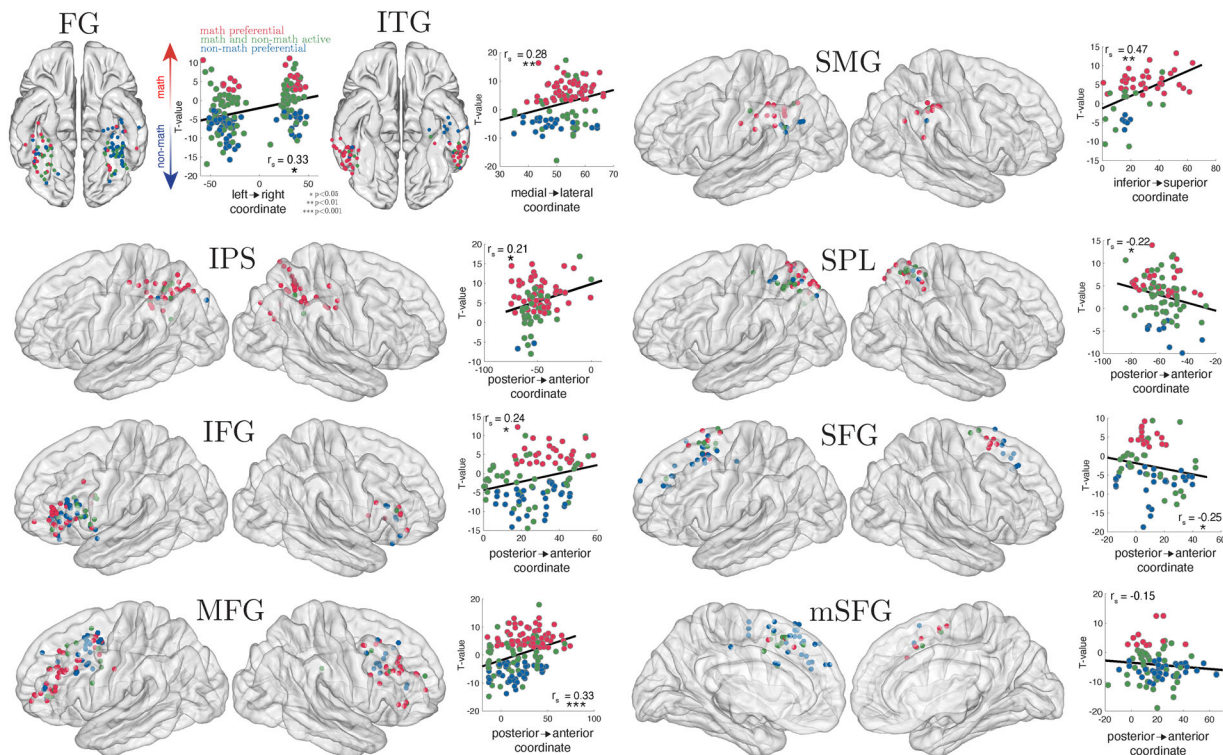

Figure 2. Anatomical localization of the preferential sites in the main nine hubs of the math network, combining the simultaneous and sequential calculation tasks. The individual electrodes in the brain are plotted in standard MNI coordinates, while in the scatterplots they are from the individual's anatomical space. The scatterplots show the correlation between the t scores comparing math versus non-math and the particular coordinate within each hub that best segregates between math and non-math preference in the native individual anatomical space. The correlation significance was FDR corrected for multiple comparisons, considering the 36 comparisons (9 regions × 4 coordinate axes, left/right, medial/lateral, posterior/anterior, and inferior/superior). This anatomical relationship may not be as clear once individual subject's data are transferred to standard MNI space. FG, fusiform gyrus; ITG, inferior temporal gyrus; SMG, supramarginal gyrus; IPS, inferior parietal sulcus; SPL, superior parietal lobe; IFG, inferior frontal gyrus; SFG, superior frontal gyrus; MFG, middle frontal gyrus; mSFG, medial superior frontal gyrus. See Extended Data Figures 1-4, 1-5, and 1-6.

the brain is yet to be engaged in arithmetic processing. The brain starts calculating when the second operand (in this case "3") is shown. The profile of activity in math-preferential sites was in sharp contrast to the profile of non-preferential sites such as early visual areas or sensory motor cortices (Fig. 3).

In parallel to activations during arithmetic processing, we found sites that showed clear decreased activity during the math condition ($n = 275$ across 46 subjects). That is, the HFB activity was reduced significantly below the baseline period, in both simultaneous and sequential calculation tasks (Fig. 4). The deactivated sites were also anatomically consistent across subjects and located in the posteromedial cortex ($n = 36\%$, 13.4%), medial temporal gyrus ($n = 37\%$, 13.4%), orbitofrontal cortex ($n = 20\%$, 7.2%), SFG ($n = 15\%$, 5.4%), superior temporal sulcus ($n = 13\%$, 4.7%), and the medial prefrontal cortex ($n = 13\%$, 4.7%)—all of which are known to be regions of the default mode network (Yeo et al., 2011). Importantly, regions with decreased activity

for math also showed the strongest signal decreases after the second operand at the same time that the math-preferential sites showed the highest activations—possibly suggesting a synchronous antagonistic relationship across the math-preferential and math-deactivated sites.

Temporal order
We calculated the concentration of HFB signal throughout each trial for each site with preferential math responses ($n = 248$, across 48 subjects) in the math condition of the simultaneous calculation task. Since the task was self-paced and trials had varying RTs within and across subjects, we normalized the HFB power by the % RT at each single trial (i.e., calculating the HFB power in the 0–100% time window of each trial). By comparing the temporal profiles of average HFB concentration across sites (Fig. 5b), a clear order of activation emerged: sites were "ignited" in a successive order. Interestingly, the earlier activations did not
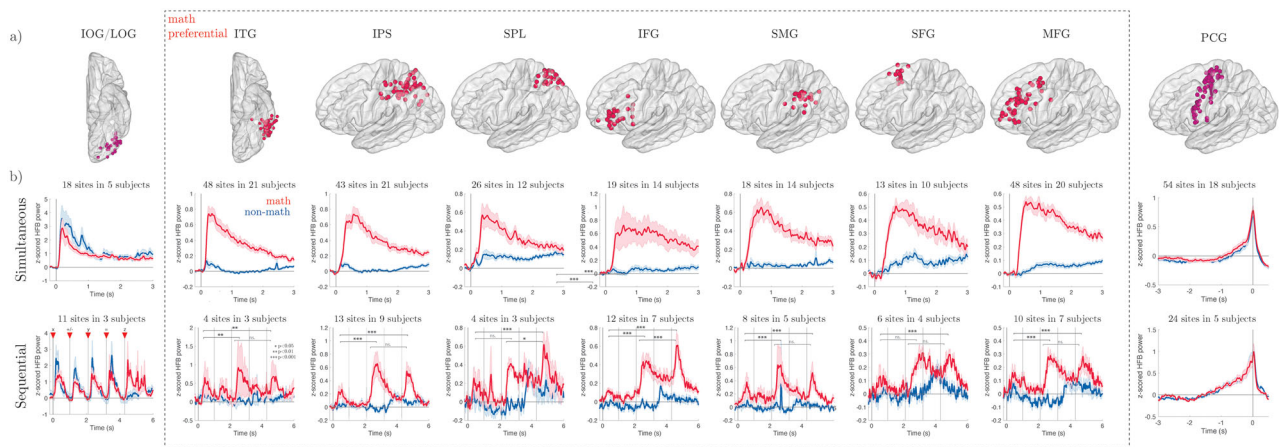

Figure 3. Profile of electrophysiological activity across the arithmetic network. **a**, Electrode localization of the main seven regions that show the strongest math selectivity in both simultaneous and sequential calculation tasks (inside the dotted line), as well as two control regions that show no math selectivity (generic visual activations in the lateral occipital cortex and motor activations in the PCG). **b**, HFB time courses for the simultaneous and sequential calculation tasks. Shaded error bars indicate the standard error of the mean across electrodes. The timing of each individual stimuli of the sequential calculation task are marked in the leftmost plot. IOG, inferior occipital gyrus; LOG, lateral occipital gyrus; PCG, precentral gyrus. See Movies 1 and 2.
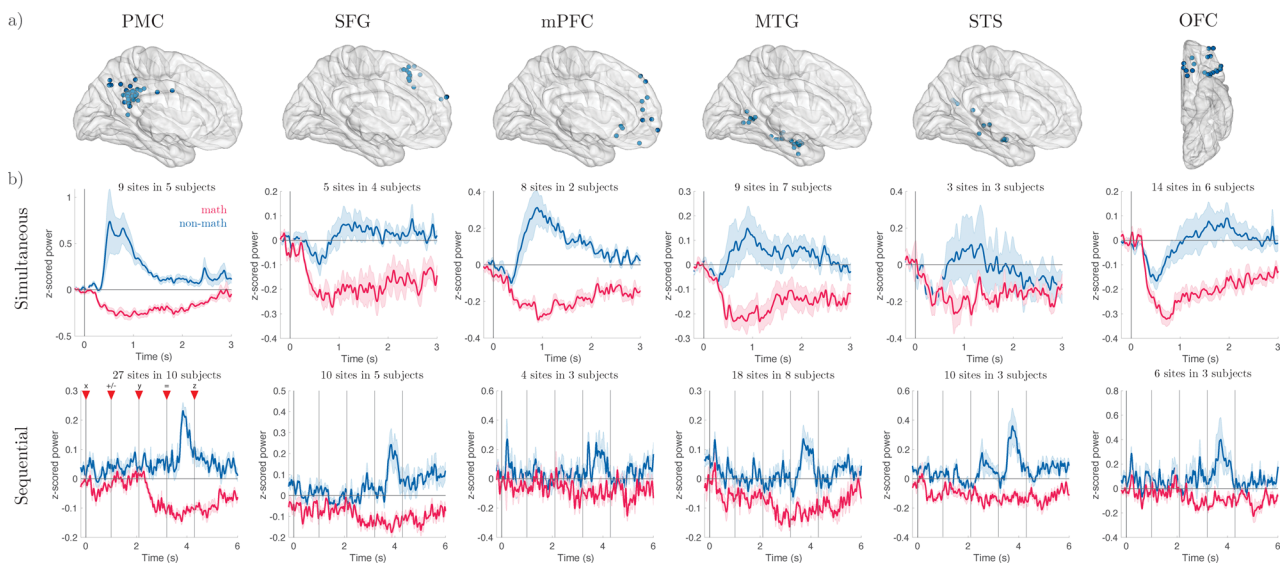

Figure 4. Profile of electrophysiological activity of regions that were deactivated during math. **a**, Electrode localization of the main six regions that show the strongest math decreased activity in both simultaneous and sequential calculation tasks. **b**, HFB time courses for the simultaneous and sequential calculation tasks. Shaded error bars indicate the standard error of the mean across electrodes. The timing of each individual stimuli of the sequential calculation task are marked in the leftmost plot.

cease when the next batch of sites were "turned on." The earlier sites continued their activity simultaneously with the later ones until all sites ended their activity as the subject responded (Fig. 5b,c).

Next, we measured the precise time of onset of HFB activations (ROL) at each site. At the group level, we observed a very clear linear trend. Activations start in the temporal lobe sites and then parietal sites before the frontal areas are engaged (Fig. 5b,c). This was confirmed with Spearman's rank correlation ($r_s = 0.52$; $p < 0.001$). In this analysis, we sought to statistically demonstrate a linear trend in the data after sorting the regions by mean ROL. Note that the purpose of this analysis was not to establish the order itself (which would be circular) but rather to confirm the presence of a statistically significant linear trend in the sorted data. To verify this finding at the single subject level, we found 16 subjects who had simultaneous recordings in at least three of the ROIs. For each participant, the order of ROIs was determined based on the group average, employing a leave-one-out strategy to circumvent a potential bias. This entailed recalculating the group mean for the ROI sequence while excluding the data of the individual participant under review. Such an approach ensured that the assessment of temporal order consistency was not compromised by the influence of an individual's data on the group analysis. Notably, the application of this method revealed a consistent ROI sequence information across all available ROIs in 15 of 16 (94%) cases. When excluding one single subject's data, the temporal sequence was changed only for the last pair of ROIs, namely, mSFG preceding the SFG. In other words, the sequence of other ROIs remained exactly the same even with inclusion of this subject. It is crucial to clarify that this single subject's data was not removed from the group dataset in its entirety. The exclusion was only specific to the analysis affected by the unusual ordering, with all other analytical aspects retaining this participant's information. This individual's data contributed to the 15 other iterations of leave-one-out procedure, reinforcing the robustness and validity of the temporal

order consistency reported across our study cohort. Next, we fit a linear regression model on the ROLs as a function of sorted ROIs. We found that the slopes of temporal order within each individual were all positive and remarkably consistent (mean, 13.3 ms; SD, 11.3 ms; R^2 of the linear fit ranged from 0.35 to 0.99; mean, 0.66; SD, 0.24) irrespective of the particular set of simultaneous ROIs recorded (Fig. 5a).

In order to probe if the temporal sequence of activations could be captured at the single-trial level, which would reflect coordinated activity across regions, we selected a single subject who had simultaneous coverage in not only ITG, IPS, and mSFG but also early visual areas [lateral occipital gyrus (LOG), posterior SPL (pSPL), as well as the precentral gyrus (PCG)]. For each electrode pair, we ran a cross-correlation analysis and estimated the indices of functional connectivity (Δr_{peak}) and temporal delay (Δr_{lag}; see Materials and Methods). If two regions are synchronized, the Δr_{peak} should be high and positive, and if one region A is leading and another region B is lagging, Δr_{lag} should be positive. As seen in Figure 6a, the early visual region (LOG), despite being the first in the cascade of activations and despite showing a significantly high initial response for arithmetic stimuli, does not show synchronized responses with downstream regions. However, the arithmetic ROI sites of ITG, IPS, and mSFG show strong evidence of synchronization with each other. The activity in these sites also correlated with the activity of subsequent regions in the processing chain even if their activity was later and aligned with the time of the subject's response (i.e., anterior SPL and the PCG in the motor cortex). These correlations clearly show a progressive lag following the processing chain order as revealed by the ROL analysis. Interestingly, we observed a decreased functional connectivity across pairs of brain regions as their temporal lag widened. In other words, as the temporal lag and order between two regions increase, their functional connectivity decreased: ITG with IPS ($\Delta r_{lag} = 4$ ms; $\Delta r_{peak} = 0.20$), mSFG ($\Delta r_{lag} = 70$ ms; $\Delta r_{peak} = 0.15$), pSPL ($\Delta r_{lag} =$
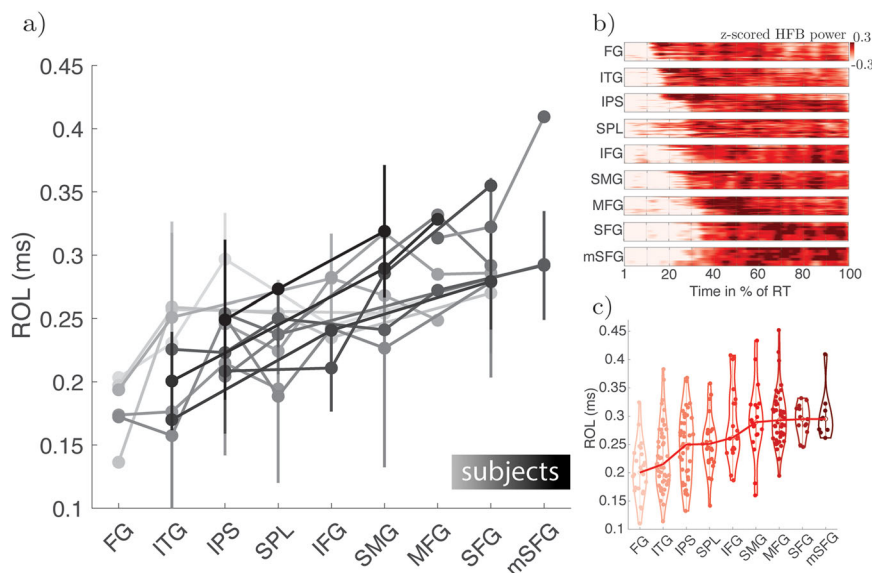

Figure 5. Temporal dynamics of math processing across regions within individual brains. *a*, In 15 subjects, we had simultaneous coverage in at least three of the nine ROIs. Each line (with a shade of gray) represents a single subject. While subjects had dissimilar coverage across the nine ROIs, it is noteworthy that the slope of the linear regression is preserved for all subjects—independently of the particular group of ROIs covered in each individual brain. Error bars indicate the standard error of the mean. *b*, RTs were normalized across subjects, and the power of HFB was plotted for each region. Each row within each matrix represents the averaged signal across trials of individual electrode sites within each anatomical region. These sites have been sorted according to their average ROL. One can clearly see a correspondent progression of time of onset of the HFB activity (i.e., ROLs) across regions. *c*, The distribution of ROL values recorded for each of the nine ROIs across subjects is shown in violin plots with dots representing an averaged ROL of a single electrode across all math trials. See Movie 1.
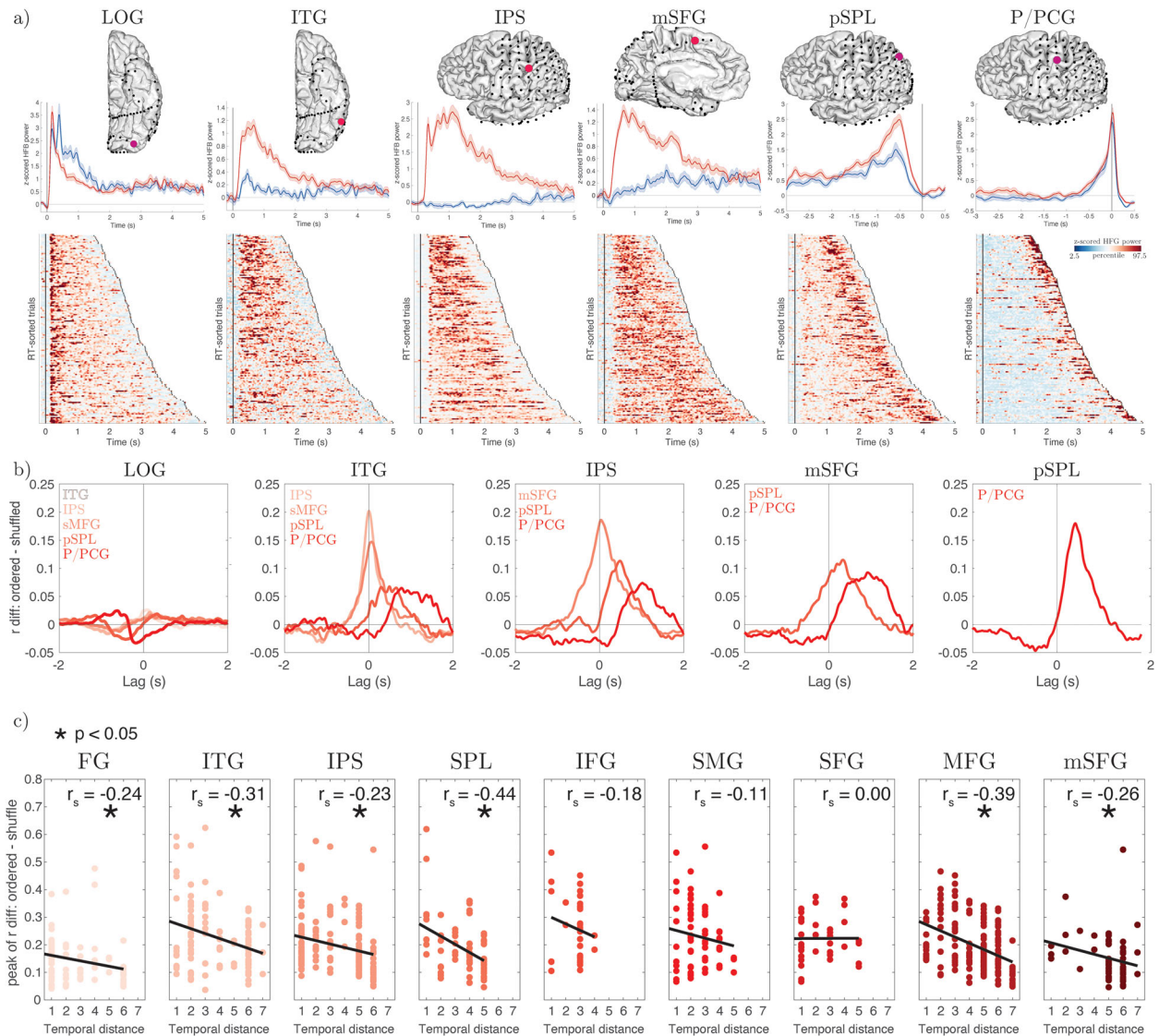
Figure 6. Functional connectivity of the main math ROIs. ***a***, Exemplar subject with simultaneous coverage of five regions activated during math, from earlier visual to the motor cortex. ITG, IPS, and mSFG showed strong math selectivity. Top time courses show averaged activity across trials for math and memory. Bottom plots show single trial activity ordered by RT (trial ends when subject presses the response button). Shaded error bars indicate the standard error of the mean across electrodes. ***b***, The same exemplar subject: lagged correlation between the activated regions. The lines represent the pairwise correlation coefficient with preserved trial order subtracted from the average correlation from the distribution of 2,000 pairwise correlations generated by shuffling the trial order. The difference between correlation values from ordered and shuffled data informs how the regions are functionally connected at the single-trial level. Rightward peaks mean that correlations are delayed. ***c***, Electrophysiological functional connectivity based on lagged correlation for each math-preferential/math-selective ROI with all the other regions, grouped using the temporal distance between them, calculated from the ROL analysis.

490 ms; $\Delta r_{peak} = 0.07$), and PCG ($\Delta r_{lag} = 788$ ms; $\Delta r_{peak} = 0.06$); IPS with mSFG ($\Delta r_{lag} = 36$ ms; $\Delta r_{peak} = -0.18$), pSPL ($\Delta r_{lag} = 486$ ms; $\Delta r_{peak} = 0.11$), and PCG ($\Delta r_{lag} = 1.01$ ms; $\Delta r_{peak} = 0.07$); mSFG with pSPL ($\Delta r_{lag} = 332$ ms; $\Delta r_{peak} = 0.11$) and PCG ($\Delta r_{lag} = 920$ ms; $\Delta r_{peak} = 0.09$); and pSPL–PCG ($\Delta r_{lag} = 436$ ms; $\Delta r_{peak} = 0.18$). To replicate what we had observed in the exemplar single subject and to probe if the pattern of electrophysiological correlation was reproducible across subjects, we calculated the degree of cross-correlation across pairs of electrodes located between any of the nine regions of interest. We found 219 pairs of electrodes with math-preferential responses in 29 subjects who had simultaneous recordings across some (but not all) nine regions of interest. Note that we used all pairs of electrodes to maximize the dataset, so, for example, if a given subject had two electrodes in the IPS and one in ITG, we included the pairs IPS_1-ITG and IPS_2-ITG. Next, we plotted the degree of correlation for a given ROI to all the other ROIs ordered by temporal distance based on the ROL measures. Next, we conducted a Spearman's rank correlation to investigate the relationship between the peak difference in correlation coefficients (ordered–shuffled trials) and the temporal order of the ROIs. The p values were FDR corrected for the nine ROIs. This analysis revealed that for most ROIs (six out of nine), there was a significantly stronger correlation between pairs of electrodes that were temporally adjacent and the strength of connectivity decreased with temporal distance across pairs of regions. In two (IFG and SMG) regions in which this tendency did not reach statistical significance, the correlation coefficient was also negative, suggesting a similar but weaker effect.

Exploring feature-dependent change of activity

Although our experiments were not designed to decipher the contribution of each brain region in specific cognitive aspects

of arithmetic processing (i.e., which region is contributing to what), we performed an exploratory analysis as an attempt to model the activity of each math-active site with a stepwise multiple linear regression—using the HFB activity as the dependent variable and several arithmetic "features" as predictors. We only used data from the sequential calculation task because, by design, this task isolates two distinct moments of interest: the calculation stage (following the presentation of the second operand) and the verification stage (following the presentation of the proposed result). For instance in $3 + 4 = 8$, the calculation stage only begins after the second operand "4" is shown, and the verification process only begins after the result "8" is presented.

We explored the effects of the five main arithmetic features that had significant impact on the measure of RT. These can be seen as indirect indices of "problem difficulty": min operand, max operand, cross-decade, format, and absolute deviant (see above, Behavioral performance). In brief, min operand is the smallest operand, the max operand is the largest operand, cross-decade means that the product of a calculation is above the decade of max operand, format refers to digit versus number word, and absolute deviant is the difference between the correct answer and the one presented in the equation.

During the calculation stage, we found that the HFB power in 55 recording sites was modulated by the min operand effect and the majority of these sites (64%) also displayed preferential responses to math compared with non-math condition (Fig. 7). Max operand and cross-decade features also modulated the HFB responses in several sites, with the majority of sites showing higher HFB activity with higher min operand (78%), max operand (92%), and equations with a cross-decade (72%). Only a small proportion of these sites showed preferential responses for math. The format modulated 93 sites, but only a minority (31%) showed preferential responses for math, suggesting that majority of math-preferential sites are format independent and that other areas related to visual processing and language contain a large number of sites modulated by digits versus number words, which might have little to do with calculation per se. Among these sites, 61% had higher activation for number words compared with digits. Finally, as expected, no site showed significant modulation by the absolute deviant, since that information is not available at the calculation stage. During the verification stage, 55 sites (44% math preferential) were modulated by the absolute deviant, with the majority responding stronger for increased magnitude of the deviant (64%).

Discussion

Our present study complements the prior imaging studies (Venkatraman et al., 2005; Amalric and Dehaene, 2016, 2017;

Mathieu et al., 2017; Yang et al., 2017) by providing hitherto unknown information about the timing of events in the brain during arithmetic processing. We recorded from a large number of sites in a large number of human subjects while they performed two arithmetic tasks. We validated the data between the two tasks and across individual subjects with recordings in the same regions of the brain. We then characterized, for the first time, the precise temporal dynamics of distributed but anatomically precise responses across coactivated neuronal populations in the human brain. This novel information will advance our understanding of the timing of events across multiple regions of the brain and will address some of the key open questions as detailed below.

Activity of a very large mantle of the human brain is changed when we engage in simple arithmetic

Subtractive approaches often used in neuroimaging methods contrast responses during a target condition with responses during the non-math condition. This subtractive method often segregates different regions of the brain and makes it impossible to differentiate conditions that lead to similar changes in activity from conditions that lead to no change in activity. Here, we compared the activity of specific populations of neurons (i.e., sites of recordings) during the math condition with their own activity a few hundred milliseconds prior to the onset of the math condition (i.e., baseline). We observed 45% of all recording sites across 85 subjects showing a significant activity. The engagement was distributed across virtually all sampled brain regions and in both hemispheres, and, interestingly, while 80% of the involved sites showed increased activity during arithmetic tasks compared with those during the baseline period, 20% displayed decreased activity. Our results demonstrate that arithmetic processing is highly distributed in the human brain, which better aligns with a more recent understanding of brain functions (Westlin et al., 2023) and corroborates many prior observations with noninvasive neuroimaging studies suggesting a widespread activation of the brain if one considers the baseline activity (rather than a different cognitive function) as a control condition. These findings impose constraints on localizationist models of mathematical processing that remain the most influential in the literature (Dehaene and Cohen, 1995; Dehaene et al., 2003). Our results suggest a broader landscape of brain regions participating in mathematical cognition than previously acknowledged. This includes not only areas demonstrating activation in response to mathematical stimuli but also regions manifesting deactivation. This diverse array of responses underscores the complexity and intricacy of the brain's processing mechanisms for mathematics, suggesting that our understanding of these processes needs to
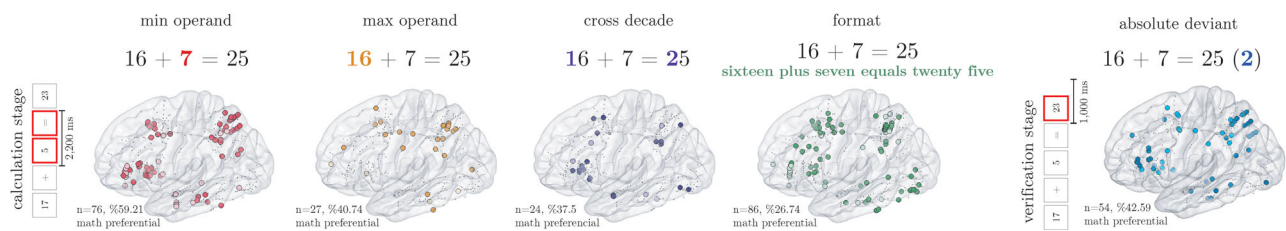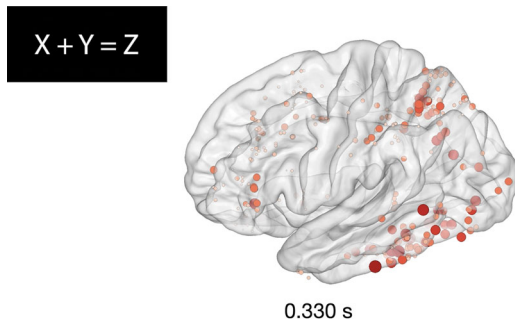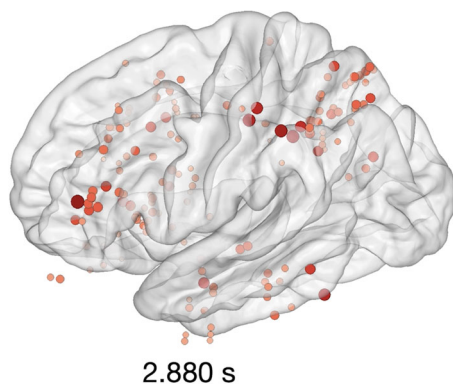

Figure 7. Encoding of arithmetic features across the math-active sites during the sequential arithmetic task. Large and colored dots represent sites in which a given feature significantly explained variance of the HFB activity (after second operand) and therefore were retained by the stepwise multiple regression fit. The darker color for min operand, max operand, and absolute deviant represents sites in which the HFB activity increased with the magnitude of these features, whereas the lighter color represents sites in which the HFB activity decreased with the magnitude of these features. For cross-decade, darker color represents sites in which the HFB activity was stronger for problems that crossed a decade (sites with the opposite effect are shown in lighter color). For format, darker color represents sites in which the HFB activity was stronger for number words as compared with digits (sites with the opposite effect are shown in lighter color).

Movie 1. Spatiotemporal activations of the simultaneous calculation task. In the simultaneous calculation task, subjects judged the accuracy of full arithmetic equations presented in X + Y = Z format (e.g., 16 + 8 = 22). This video shows how the power of activity in the HFB changes from ∼100 ms before until ∼1000 ms after the stimulus onset in select electrodes with preferential activity during the math condition. [view online]

Movie 2. Spatiotemporal activations of the sequential calculation task. Same as Movie 1, but the responses are measured during the sequential calculation task, when subjects viewed math stimuli appearing sequentially one at a time in "X", "+", "Y", "=", "Z" format (e.g., "16", "+", "8", "=", "22"). [view online]

consider a more holistic and interconnected network of regions rather than isolated localized areas.

Math-preferential and non-math–preferential sites are orderly colocalized

To make a bridge to the neuroimaging literature, we then employed a subtractive method (akin to the ones used in neuroimaging studies) and found nine regions with significantly higher responses during the target (i.e., math) condition. The anatomical location of these sites was remarkably consistent across subjects and replicated the findings reported in previous fMRI studies, namely, FG, ITG, IPS, SPL, SMG, IFG, MFG, SFG, and mSFG. In our analysis, we defined the preferentiality of responses by the presence of significant activation during the math condition and no activations during the control condition. However, we emphasize that the set of regions showing preferential responses during the math condition may not represent a "selective" math network as their preferential response during the math condition compared with that during non-math condition does not imply that they are solely involved in arithmetic processing. In keeping with this, we recently showed that electrodes in the PPC with preferential responses to math also showed preferential responses to visuospatial cues appearing in the contralateral, but not ipsilateral, visual fields (Liu et al., 2021). Furthermore, as we discuss later, our multiple regression analysis revealed that the encoding of different arithmetic features is

distributed across brain regions and is not limited to the sites with strongest math-preferential responses.

A potential confound for the selectivity analysis is related to the possibility that the math condition may have generally been more demanding for some subjects. Nevertheless, we posit that the task demand is not the solitary determinant and present two reasons to substantiate this claim. First, as elucidated in our reaction time analyses, an interesting pattern emerged. We observed higher RT for the math condition when compared with that for the non-math condition in the simultaneous task. Yet, a reverse pattern was notable in the sequential task, where the non-math condition yielded higher RT in comparison with the math condition. Secondly, our approach to identifying a site as "math preferential" was predicated on three specific criteria. The site needed to exhibit a significantly higher HFB activity during math trials as compared with the baseline and a higher trial HFB activity during the math condition in relation to the non-math condition. Of paramount importance, though, was the third criterion: the site was not allowed to show a significant difference in trial HFB activity during the non-math condition when compared with that during the baseline. The third criterion is particularly salient, given that task demand was also a component in the non-math (memory) condition, albeit to a lesser extent. Rather than reporting a "graded" response, we observed that the math-preferential sites demonstrated no responses during the non-math condition. This rigorous definition bolsters our belief that the observed preferential responses are, in large measure, driven by the task content.

Neuroimaging studies often highlight a set of brain regions with increased hemodynamic responses during a target condition. Such group-based findings may be misinterpreted as if the entire region is homogeneously activated during the target condition across individual brains. Our findings provided a glimpse of functional organization in the human brain in the mesoscale (millimeter) level. Neuronal populations with increased activations during the target math condition were found to be colocalized adjacent to populations with preferential responses during the nontarget (memory) condition and that neuronal populations with opposite profiles of activity were orderly colocalized; that is, anterior proclivity for math preferentiality was seen in IPS, MFG, and IFG; posterior proclivity in SPL and SFG; dorsal proclivity in the SMG; and right hemispheric proclivity in the FG. In other words, adjacent populations of neurons that are anatomically juxtaposed with each other may have preferentiality for different cognitive functions. That might explain why neuropsychological patients almost always display a variety of cognitive deficits spanning different cognitive functions, following a lesion or atrophy in specific brain regions (Baldo and Dronkers, 2007; Gorno-Tempini et al., 2011). Our results indicate that some brain regions may indeed be engaged in both mathematical and linguistic processes and that these cognitive symbolic systems could share some underlying computational mechanisms. This perspective aligns with a growing body of evidence pointing toward the overlap in neurodevelopmental disorders, reinforcing the idea that these disorders are complex, multifactorial entities that often manifest in a spectrum of probabilistic subtypes (Pennington, 2006). It is noteworthy that estimates suggest up to 40% of children with dyscalculia (mathematical deficits) also exhibit symptoms of dyslexia (reading deficits; Skeide, 2022). Therefore, our findings underscore the need to move beyond a compartmentalized view of cognitive functions and toward a more integrated understanding of the brain activity.

Although our study did not specifically formulate hypotheses regarding the within-region anatomical organization of juxtaposed activations, we believe our findings provide a robust foundation for future research. This body of work could delve deeper into the intricate anatomical structuring associated with high-level cognitive functions, thereby advancing our understanding of cerebral organization.

Successive engagement and recurrent interactions

One of the most important findings in our study pertains to our observation of temporally ordered successive "ignition" of brain regions during a simple arithmetic function at the single-subject level. As noted, a much larger extent of the brain was activated during the math condition. However, by focusing on the select sites of interest (i.e., nine anatomical regions with math-preferential responses), we explored the temporal order of activation across regions and found a successive order of activations, within the subsecond space, from FG to ITG, IPS, SPL, IFG, SMG, MFG, lateral SFG, and lastly mSFG sites (Fig. 5b,c). More importantly, distinct regions of the brain became engaged and remained engaged above their own baseline across the length of each trial until the subject responded. It should be noted that our finding of temporal order of activations was not an artifact of averaging across different brains. As clearly documented in Figure 5a, in 15 subjects with simultaneous recording across several of the same ROIs, a similar temporal order and slope were observed. Across subjects, the coefficient of this temporal order was nearly identical even though each subject performed the task with variable RTs.

Our observations from the cross-correlational analysis showed that the temporal precedence of activation was not sufficient to influence the activity profile of the rest of the chain of regions. Instead, regions that are temporally closer to each other seem to be more strongly influencing each other at the single-trial level. As regions get further apart in temporal order, their degree of influence decreases. For instance, in an exemplar subject with simultaneous coverage in multiple math-preferential regions, we found a very weak degree of connectivity between the first and the rest of the regions that responded. However, we observed a strong functional relationship (with an expected temporal lag) between the ITG and IPS.

Although the aim of the current study was not to arbitrate between different architectures of information processing in the brain, our real brain data can be taken as a support of previously proposed theoretical models such as the ordered and functionally dependent cascade of partially overlapping brain states (McClelland, 1979). Our observation that the information gets progressively lost or transformed along the processing chain also supports theoretical models such as the leaky competing accumulator model (Usher and McClelland, 2001). The notion of "information leak" in cognitive processing alludes to the imperfect retention or utilization of information essential for the task performance at each step in the processing chain. This may occur due to either the imperfect transmission of information from one brain region to another or because a brain region does not fully utilize the information it receives. Several factors could contribute to this "leakage," such as inherent noise in neural signaling, the complexity of the information being processed, or limitations in the brain's computational capacity (Bernacchia et al., 2011). From a neurophysiological perspective, these information leaks or transformations could manifest through various mechanisms, for instance, the decay or dispersion of the neural signal as it travels between the brain regions or the selective filtering of information based on the task relevance (Kiebel et al., 2008). Moreover, the transformation of information could refer to how information is repackaged or reformatted across different regions or processing stages. Initial processing stages may involve encoding the basic numerical data or mathematical operations. In contrast, later stages could involve more complex processes like error checking, problem-solving strategy selection, or the integration of numerical data with spatial, temporal, or other contextual information. Consequently, the same piece of information could take on different forms or representations as it progresses along the processing chain.

Overall, our findings are in line with a growing literature that proposes that even simple tasks like object recognition (Kar et al., 2019), visibility judgment (King et al., 2016), and hierarchical perceptual decisions (Gwilliams and King, 2020) involve a distributed network of recurrent interactions, beyond purely feedforward architectures (Lamme and Roelfsema, 2000). Our work expands on these findings from very simple operations and suggests that a similar architecture underlies the processing of complex human-unique abilities such as symbolic arithmetic.

Relating the spatiotemporal dynamics of brain activity to specific stages of cognitive processing

While the current study was not designed to address the neural mechanisms underlying specific stages of cognitive processing during the target condition (i.e., mathematical processing), our data revealed important layers of information that can guide future mechanistic explorations. For instance, we observed a clear profile of activations with higher HFB activity primarily following the second operand and after the presentation of the equation results. These time points are precisely the times in which subjects become engaged in arithmetic calculation and comparison between the correct and presented results. Interestingly, in the sites deactivated during the arithmetic condition, we discovered that the onset of such decreased activity occurred after the presentation of the second operand matching (and coinciding in time with) the sharp activations in the functionally opposing regions. These observations were remarkably reproducible across subjects and consistent with our own preliminary findings in a few regions of the brain (Daitch et al., 2016; Baek et al., 2018; Hermes et al., 2017). Moreover, by manipulating the format of presentation (digits vs number words), we showed that the majority of the math-preferential sites are agnostic about the specific format in which the numbers are presented and therefore operate on an abstract level.

We should clarify that our current tasks were not specifically tailored to examine the discrete role of each brain region during mental calculations. Therefore, our findings should be viewed as an initial foray toward a comprehensive and precise spatiotemporal dissection of the computations performed at individual brain sites during arithmetic processing. One noteworthy finding from our multiple regression analysis suggests a distributed encoding of different cognitive features, challenging the notion that these features are confined solely to regions displaying preferential responses during the target condition.

These observations do not just question prevailing notions of brain functional organization; they also challenge established models of arithmetic processing, such as Dehaene and colleagues' triple-code model (Dehaene and Cohen, 1995). In these models, specific functions related to numerical and arithmetic processing are assigned to each area within the potential math network. However, our study unveils a more distributed pattern of the brain region engagement during mental calculations, which

does not align perfectly with the functional compartmentalization proposed by models like the triple-code model.

Our results thus call for a re-evaluation of traditional models of arithmetic processing and underscore the necessity for further research incorporating a more distributed conception of the brain function. Future iEEG studies, with targeted experimental tasks, ought to employ a whole-brain level of analysis to decipher the contribution of each brain region of interest in specific features of the arithmetic condition.

Closing remarks

Our large-scale anatomical, temporal, and functional iEEG findings provide novel information about the profile of neural activity across different regions of the human brain to help characterize how different regions of the brain work collectively in the service of a given task. As such, the present work ought to be taken as a prototype model for how different anatomical populations in distinct regions of the brain change their activity in unison with each other to enable a human subject to perform a cognitive task as simple as $2 + 2 = 4$. We hope that our findings, along with the acquired raw data, which will be shared in a public repository, can be used as a real brain data to construct more accurate theoretical models of distributed brain activity.

Data Availability Statement

The dataset will be shared upon request. All code to preprocess, analyze, and visualize the data is available at https://github.com/pinheirochagas/lbcn_preproc.

References

Amalric M, Dehaene S (2016) Origins of the brain networks for advanced mathematics in expert mathematicians. Proc Natl Acad Sci U S A 113: 4909–4917.

Amalric M, Dehaene S (2017) Cortical circuits for mathematical knowledge: evidence for a major subdivision within the brain's semantic networks. Philos Trans R Soc Lond B Biol Sci 373:20160515.

Ansari D (2008) Effects of development and enculturation on number representation in the brain. Nat Rev Neurosci 9:278–291.

Baek S, Daitch AL, Pinheiro-Chagas P, Parvizi J (2018) Neuronal population responses in the human ventral temporal and lateral parietal cortex during arithmetic processing with digits and number words. J Cogn Neurosci 30:1315–1322.

Baldo JV, Dronkers NF (2007) Neural correlates of arithmetic and language comprehension: a common substrate? Neuropsychologia 45:229–235.

Barrouillet P, Thevenot C (2013) On the problem-size effect in small additions: can we really discard any counting-based account? Cognition 128:35–44.

Benjamini Y, Hochberg Y (1995) Controlling the false discovery rate: a practical and powerful approach to multiple testing. J R Stat Soc Series B Methodol 57:289–300.

Bernacchia A, Seo H, Lee D, Wang XJ (2011) A reservoir of time constants for memory traces in cortical neurons. Nat Neurosci 14:366–372.

Brannon EM (2006) The representation of numerical magnitude. Curr Opin Neurobiol 16:222–229.

Butterworth B, Walsh V (2011) Neural basis of mathematical cognition. Curr Biol 21:R618–R621.

Cantlon JF, Platt ML, Brannon EM (2009) Beyond the number domain. Trends Cogn Sci 13:83–91.

Cohen Kadosh R, Dowker A (2015) The Oxford handbook of numerical cognition. New York: Oxford Press.

Daitch AL, Foster BL, Schrouff J, Rangarajan V, Kasikci I, Gattas S, Parvizi J (2016) Mapping human temporal and parietal neuronal population activity and functional coupling during mathematical cognition. Proc Natl Acad Sci U S A 113:201608434.

Dehaene S (2011) The number sense: how the mind creates mathematics, Ed. 2. New York: Oxford University Press.

Dehaene S, Cohen L (1995) Towards an anatomical and functional model of number processing. Math Cogn 1:83–120.

Dehaene S, Piazza M, Pinel P, Cohen L (2003) Three parietal circuits for number processing. Cogn Neuropsychol 20:487–506.

Dehaene S, Spelke E, Pinel P, Stanescu R, Tsivkin S (1999) Sources of mathematical thinking: behavioral and brain-imaging evidence. Science 284: 970–974.

Delazer M, Domahs F, Bartha L, Brenneis C, Lochy A, Trieb T, Benke T (2003) Learning complex arithmetic–an fMRI study. Brain Res Cogn Brain Res 18:76–88.

De Smedt B, Holloway ID, Ansari D (2011) Effects of problem size and arithmetic operation on brain activation during calculation in children with varying levels of arithmetical fluency. NeuroImage 57:771–781.

Dubey A, Ray S (2019) Cortical electrocorticogram (ECoG) is a local signal. J Neurosci 39:4299–4311.

Dykstra AR, Chan AM, Quinn BT, Zepeda R, Keller CJ, Cormier J, Madsen JR, Eskandar EN, Cash SS (2012) Individualized localization and cortical surface-based registration of intracranial electrodes. NeuroImage 59: 3563–3570.

Fischl B, Sereno MI, Dale AM (1999) Cortical surface-based analysis. II: Inflation, flattening, and a surface-based coordinate system. NeuroImage 9:195–207.

Gorno-Tempini ML, et al. (2011) Classification of primary progressive aphasia and its variants. Neurology 76:1006–1014.

Grabner RH, Ischebeck A, Reishofer G, Koschutnig K, Delazer M, Ebner F, Neuper C (2009) Fact learning in complex arithmetic and figural-spatial tasks: the role of the angular gyrus and its relation to mathematical competence. Hum Brain Mapp 30:2936–2952.

Grabner RH, Ansari D, Koschutnig K, Reishofer G, Ebner F (2013) The function of the left angular gyrus in mental arithmetic: evidence from the associative confusion effect. Hum Brain Mapp 34:1013–1024.

Greve DN, Fischl B (2009) Accurate and robust brain image alignment using boundary-based registration. Neuroimage 48:63–72.

Groen GJ, Parkman JM (1972) A chronometric analysis of simple addition. Psychol Rev 79:329–343.

Groppe DM, Bickel S, Dykstra AR, Wang X, Mégevand P, Mercier MR, Lado FA, Mehta AD, Honey CJ (2017) iELVis: an open source MATLAB toolbox for localizing and visualizing human intracranial electrode data. J Neurosci Methods 281:40–48.

Grotheer M, Ambrus GG, Kovacs G (2016a) Causal evidence of the involvement of the number form area in the visual detection of numbers and letters. NeuroImage 132:314–319.

Grotheer M, Herrmann K-H, Kovacs G (2016b) Neuroimaging evidence of a bilateral representation for visually presented numbers. J Neurosci 36:88–97.

Grotheer M, Jeska B, Grill-Spector K (2018) A preference for mathematical processing outweighs the selectivity for Arabic numbers in the inferior temporal gyrus. NeuroImage 175:188–200.

Gwilliams L, King JR (2020) Recurrent processes support a cascade of hierarchical decisions. Elife 9:e56603.

Harvey BM, Klein BP, Petridou N, Dumoulin SO (2013) Topographic representation of numerosity in the human parietal cortex. Science 341:1123–1126.

Harvey BM, Ferri S, Orban GA (2017) Comparing parietal quantity- processing mechanisms between humans and macaques. Trends Cogn Sci 21: 779–793.

Hermes D, Rangarajan V, Foster BL, King J-R, Kasikci I, Miller KJ, Parvizi J (2017) Electrophysiological responses in the ventral temporal cortex during reading of numerals and calculation. Cereb Cortex 27:567–575.

Holloway ID, Ansari D (2010) Developmental specialization in the right intraparietal sulcus for the abstract representation of numerical magnitude. J Cogn Neurosci 22:2627–2637.

Jenkinson M, Smith S (2001) A global optimisation method for robust affine registration of brain images. Med Image Anal 5:143–156.

Jenkinson M, Bannister P, Brady M, Smith S (2002) Improved optimization for the robust and accurate linear registration and motion correction of brain images. NeuroImage 17:825–841.

Kanjlia S, Lane C, Feigenson L, Bedny M (2016) Absence of visual experience modifies the neural basis of numerical thinking. Proc Natl Acad Sci U S A 113:201524982.

Kar K, Kubilius J, Schmidt K, Issa EB, DiCarlo JJ (2019) Evidence that recurrent circuits are critical to the ventral stream's execution of core object recognition behavior. Nat Neurosci 22:974–983.

Kiebel SJ, Tallon-Baudry C, Friston KJ (2005) Parametric analysis of oscillatory activity as measured with EEG/MEG. Hum Brain Mapp 26:170–177.

Kiebel SJ, Daunizeau J, Friston KJ (2008) A hierarchy of time-scales and the brain. PLoS Comput Biol 4:e1000209.

King J-R, Pescetelli N, Dehaene S (2016) Brain mechanisms underlying the brief maintenance of seen and unseen sensory information. Neuron 92: 1122–1134.

Knops A (2020) Numerical cognition. New York: Routledge.

Knops A, Thirion B, Hubbard EM, Michel V, Dehaene S (2009) Recruitment of an area involved in eye movements during mental arithmetic. Science 324:1583–1585.

Lamme VAF, Roelfsema PR (2000) The distinct modes of vision offered by feedforward and recurrent processing. Trends Neurosci 23:571–579.

Liu N, Pinheiro-Chagas P, Sava-Segal C, Kastner S, Chen Q, Parvizi J (2021) Overlapping neuronal population responses in the human parietal cortex during visuospatial attention and arithmetic processing. J Cogn Neurosci 33:2548–2558.

Logothetis NK, Pauls J, Augath M, Trinath T, Oeltermann A (2001) Neurophysiological investigation of the basis of the fMRI signal. Nature 412:150–157.

Mathieu R, Epinat-duclos J, Sigovan M, Breton A, Cheylus A, Fayol M, Thevenot C, Prado J (2017) What's behind a " + " sign? Perceiving an arithmetic operator recruits brain circuits for spatial orienting. Cereb Cortex 28:1673–1684.

McClelland JL (1979) On the time relations of mental processes: an examination of systems of processes in cascade. Psychol Rev 86:287–330.

Nieder A (2019) A brain for numbers: the biology of the number instinct. Boston: The MIT Press.

Papademetris X, Jackowski MP, Rajeevan N, DiStasio M, Okuda H, Constable RT, Staib LH (2006) BioImage Suite: an integrated medical image analysis suite: an update. Insight J 2006:209.

Parvizi J, Kastner S (2018) Promises and limitations of human intracranial electroencephalography. Nat Neurosci 21:474–483.

Pennington BF (2006) From single to multiple deficit models of developmental disorders. Cognition 101:385–413.

Piazza M, Pinel P, Le Bihan D, Dehaene S (2007) A magnitude code common to numerosities and number symbols in human intraparietal cortex. Neuron 53:293–305.

Pinheiro-Chagas P, Dotan D, Piazza M, Dehaene S (2017) Finger tracking reveals the covert processing stages of mental arithmetic. Open Mind 1: 30–41.

Pinheiro-Chagas P, Chen F, Sabetfakhri N, Perry C, Parvizi J (2022) Direct intracranial recordings in the human angular gyrus during arithmetic processing. Brain Struct Funct 228:305–319.

Pinheiro-Chagas P, Daitch A, Parvizi J, Dehaene S (2018) Brain mechanisms of arithmetic: a crucial role for ventral temporal cortex. J Cogn Neurosci 30:1757–1772.

Ray S, Maunsell JHR (2011) Different origins of gamma rhythm and high-gamma activity in macaque visual cortex. PLoS Biol 9:e1000610.

Schrouff JV, Raccah O, Baek S, Rangarajan V, Salehi S, Mourao-Miranda J, Helili Z, Daitch AL, Parvizi J (2018) Fast temporal dynamics and causal relevance of face processing in the human temporal cortex. bioRxiv.

Shum J, Hermes D, Foster BL, Dastjerdi M, Rangarajan V, Winawer J, Miller KJ, Parvizi J (2013) A brain area for visual numerals. J Neurosci 33:6709–6715.

Skeide M (2022) The Cambridge handbook of dyslexia and dyscalculia (Skeide MA, ed). Cambridge: Cambridge University Press.

Uittenhove K, Thevenot C, Barrouillet P (2016) Fast automated counting procedures in addition problem solving: when are they used and why are they mistaken for retrieval? Cognition 146:289–303.

Usher M, McClelland JL (2001) The time course of perceptual choice: the leaky, competing accumulator model. Psychol Rev 108:550–592.

Venkatraman V, Ansari D, Chee MWL (2005) Neural correlates of symbolic and non-symbolic arithmetic. Neuropsychologia 43:744–753.

Westlin C, et al. (2023) Improving the study of brain–behavior relationships by revisiting basic assumptions. Trends Cogn Sci 27:246–257.

Yang AI, Wang X, Doyle WK, Halgren E, Carlson C, Belcher TL, Cash SS, Devinsky O, Thesen T (2012) Localization of dense intracranial electrode arrays using magnetic resonance imaging. NeuroImage 63:157–165.

Yang Y, Zhong N, Friston K, Imamura K, Lu S, Li M, Zhou H, Wang H, Li K, HuB (2017) The functional architectures of addition and subtraction: network discovery using fMRI and DCM. Hum Brain Mapp 38:3210–3225.

Yeo BTT, et al. (2011) The organization of the human cerebral cortex estimated by intrinsic functional connectivity. J Neurophysiol 106: 1125–1165.